

INVITED REPORT

Class Transitions in Black Holes

Sandip K. Chakrabarti^{1,2} *

¹ S. N. Bose National Centre for Basic Sciences, Salt Lake, Kolkata, 700098, India

² Centre for Space Physics, Chalantika 43, Garia Station Road, Kolkata 700084, India

Abstract A black hole spectrum is known to change from the hard state to the soft state when the energy spectral index α ($F_E \propto E^{-\alpha}$) in, say, 2–20 keV range changes from $\alpha \sim 0.5$ to ~ 1.5 . However, this ‘classical’ definition which characterizes black holes like Cyg X-1, becomes less useful for many objects such as GRS 1915+105 in which the spectral slope is seen to vary from one to the other in a matter of seconds and depending on whether or not winds form, the spectral slope also changes. The light curves and the colour-colour diagrams may look completely different on different days depending on the frequency and mode of switching from one spectral state to the other. Though RXTE observations have yielded wealth of information on such ‘variability classes’ in GRS 1915+105, very rarely one has been able to observe how the object goes from one class to the other. In the present review, we discuss possible origins of the class transition and present several examples of such transitions. In this context, we use mostly the results of the Indian X-ray Astronomy Experiment (IXAE) which observed GRS 1915+105 more regularly.

Key words: Black hole physics – accretion, accretion disks – hydrodynamics – shock waves – stars: individual (GRS1915+105)

1 INTRODUCTION

Black holes are fundamentally ‘black’ in that they cannot be observed directly. However, the behaviour of radiation emitted by the matter falling onto them can be studied through carefully planned observations and a wealth of information about the black hole and the accretion flow could be obtained. In the present review, we concentrate on the characteristics of class transitions in black holes and infer possible physical processes which may be responsible for such transitions.

2 NATURE OF EMITTED RADIATION: THEORETICAL EXPECTATIONS

Radiations emitted from the infalling matter carry information about the density, temperature and magnetic field distribution. Theoretically, these flow variables are derived in conjunction

* E-mail: chakraba@bose.res.in

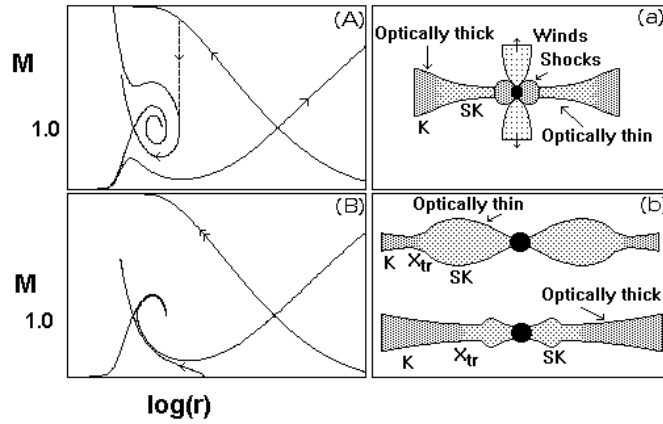


Fig. 1 Typical solutions of viscous transonic flows are shown in the left panels for (a) viscosity parameter lower than the critical value and (b) viscosity parameter above the critical value. The corresponding flow configurations are shown on the right.

with the velocity profiles (subsonic/supersonic nature) when proper hydro- and magnetohydrodynamic treatments are made. By ‘proper’, we mean by actually solving full set of equations with appropriate boundary conditions and not making ‘models’. The general picture which comes out has been discussed in several papers and we refer to some recent reviews (Chakrabarti, 1996, 2001) in this connection.

In order to re-iterate the importance of the role of transonic solutions in understanding black hole accretion process and therefore the spectral variations including the variability class transitions, we present in Fig. 1(a-b) two types of basic solutions of the viscous transonic flows (see, Chakrabarti, 1990, 1996 for details). In Fig. 1a, (upper panel) a solution with a small viscosity parameter is presented which includes a standing shock transition shown by a vertical arrow. In the left, the Mach number variation is presented and in the right, the flow configuration is presented. In the outer regions, when the flow is sub-sonic, it is more or less Keplerian (K). After the flow becomes super-sonic, the flow becomes sub-Keplerian (SK). It passes through a centrifugal force induced standing or oscillating shock and become subsonic again which enters through the inner sonic point to become super-sonic. This region between the shock and the horizon is known as the CENtrifugal pressure dominated BOUNDary Layer or CENBOL which essentially releases most of the observable X-rays in a galactic black hole accretion. When the viscosity is higher (Fig. 1b), the solution changes its character: there are now *two* solutions, one directly coming from a Keplerian disk and entering through the inner sonic point (lower branch), while the other passes through the outer sonic point before disappearing into a black hole. The configuration profiles show the essential differences. It is natural that both of these steady solutions cannot be realized simultaneously. Time dependent simulations always prefer the higher entropy solution passing through the inner sonic point. Thus while at lower viscosities, the flow forms a steady or oscillating shock, at higher viscosities the flow indeed forms a shock by staying on the upper branch, but the shock propagates away to a larger distance (Chakrabarti & Molteni, 1995) while converting the post-shock region into a Keplerian disk on its way. Thus, it ends up in the lower branch. This is how a Keplerian disk forms in the first place. Figure 2(a-b) shows this behaviour where evolution of the Mach number and the specific angular momentum are shown.

Thus we observe that both the Keplerian and the sub-Keplerian flow could be present depending on viscosity parameter and on the basis of these theoretical considerations, Chakrabarti

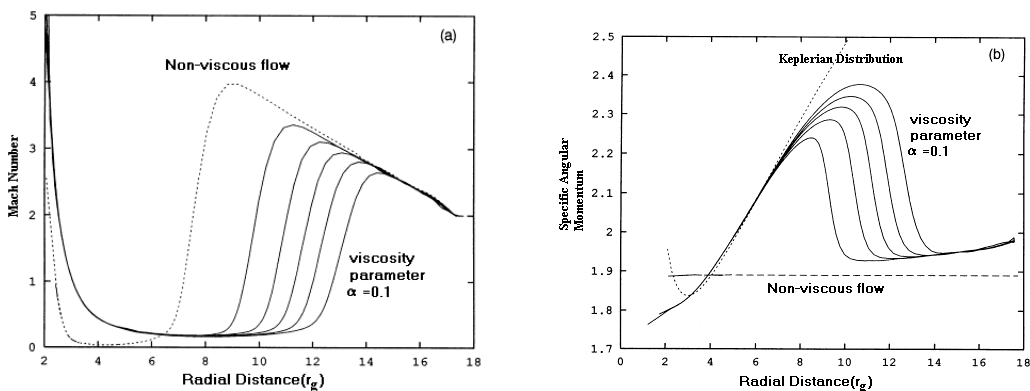


Fig. 2 Time dependent solutions of (a) the Mach number and (b) the specific angular momentum distribution of an advective flow in which viscosity parameter is above the critical value. The shock, formed closed to the black hole, propagates outward leaving behind a Keplerian disk between the shock and marginally stable orbit. Solutions without viscosity are also placed for comparison.

(1994) and Chakrabarti & Titarchuk (1995) proposed that perhaps both the components are present in a generic flow around galactic and extragalactic black holes with the Keplerian disk in the equatorial plane flanked by sub-Keplerian flows above and below. Subsequently, it was found that the CENBOL could be the source of the jets as well (Chakrabarti, 1998, 1999) and the ratio of the outflow rate to the inflow rate $R_{\text{jet}} = \dot{m}_{\text{out}}/\dot{m}_{\text{in}}$ strongly depends on the strength of the shock, characterized by the compression ratio R . In both the weak ($R \sim 0$) and the strong ($R \sim 4 - 7$) shocks, the ratio is low, while for the intermediate shocks of strength ($\sim 2 - 3$) the ratio is very high. A high R_{jet} , coupled to a high \dot{m}_{in} produces profuse amount of outflows which can influence the spectral properties in the following way: (a) the outflow, up to the sonic sphere, moves slowly and has higher optical depth. It intercepts the soft-photons from the disk and reprocesses them. If the optical depth is high enough, it can be cooled efficiently and the flow might just lose its drive to go out and fall back into the disk itself, temporarily increasing the accretion rates. Eventually, after this temporary phase is over after the viscous time scale of a few tens of seconds, the CENBOL develops once more and the outflow starts all over again. All these phases could be observable in the spectral feature and light curves which determine the ‘class’ of a black hole. (b) In case the accretion rate is not high enough, the outflow will not be cooled and would continue to propagate steadily. This type of ‘class’ may continue for a long time, unless the rates (Keplerian and sub-Keplerian) themselves are fundamentally changed at the outer edge in the first place. Change in viscosity brings rise to changes in the Keplerian/sub-Keplerian rates (see Fig. 2 above) as well.

According to this Two Component Advective Flow (TCAF) paradigm, oscillations of shocks give rise to the quasi-periodic oscillations (QPOs). Thus QPOs are possible when shocks are. But the reverse is not true, since not all the shocks are expected to oscillate (Molteni, Sponholz & Chakrabarti, 1996; Chakrabarti, Acharyya & Molteni, 2004). Shocks are also useful in accelerating particles and producing non-thermal spectra. Thus, high energy emissions may also be explained from by TCAF solution (Chakrabarti, 2004) The existence of two components in the flow has been verified observationally (Smith, Heindl & Swank, 2002).

In Fig. 3, we present a few types of configurations of the Two Component Advective Flows (TCAF) which give rise to different types of light curves. In the upper left, the sub-Keplerian component has no sharp shock transition, but the flow is puffed up due to slowing down of

matter (and becoming hotter in the process) due to the centrifugal barrier. This is expected to produce a light curve with no QPO and with a low rate of outflow. The spectrum will be harder. In upper-right, we schematically show the CENBOL as a spherical region (which in reality is a ‘thick disk’ like region with funnel etc. (see, Chakrabarti, 1993) which is formed due to a steady or an oscillating shock. Thermally/centrifugally/magneto-centrifugally driven wind comes out of this region. This configuration is expected to produce harder spectrum with a QPO with possible drifting frequency due to variation in accretion rate and viscosity. Accretion rate controls the cooling rate and hence the shock (QPO) oscillation frequency. In the lower left, we show the situation when the outflow could become optically thick and return flow causes the jets to be blobby. Return flow temporarily increases the accretion rate and soft-state may develop. This may cause switching of states at the interval of a few seconds in some of the classes. In lower-right, the viscosity is so high that the Keplerian disk reaches close to the inner sonic point (Fig. 2b) and in this soft/quasi-soft state hard spectra can be produced by the bulk motion Comptonization and radiations from non-thermal particles in accretion and wind shocks.

It is to be noted that in the TCAF solution, the advective flow itself is the Compton cloud. The literature is overwhelmed with the models such as ADAF, dynamical corona and the like which can at the best mimic the CENBOL of TCAF solution. A standing, propagating or oscillating shock close to a black hole, is not a wishful thinking, but it is a reality. The cartoon diagram may remind people of two-temperature flow of Shapiro, Lightman and Eardley (1976), but the difference is that presently one is not discussing ‘Keplerian’ advective flow as no such thing exists. Similarly, it may also remind one of thick accretion flow: this is also not correct, as the thick disk solutions are purely rotating and are not attached to any disk. The only self-consistent solutions which include thick disk like feature as well as the disk is the advective flow model presented more than ten years back (see, Chakrabarti, 1993).

In Fig. 4, we show schematically how the interactions among the disk, CENBOL and the jet components could give rise to time-dependent behaviour of the light curves (Chakrabarti et al. 2002a). Actual numerical simulation is difficult in presence of Comptonization, however using one type of cooling only, we have been able to show that the Power density spectrum of the χ state could be produced as observed (Chakrabarti, Acharyya & Molteni, 2004; see also Chakrabarti, this volume). Details of the results of this non-linear analysis will be discussed elsewhere.

3 CLASSIFICATION OF LIGHT CURVES OF GRS1915+105 AND THEIR TRANSITIONS

One of the puzzling black holes is GRS 1915+105 which exhibits large variations in the light curves. Originally these were classified into twelve classes by Belloni et al. (2000) on the basis of the hardness ratio. Naik et al. (2002) showed that there is another independent class. In Chakrabarti & Nandi (2000) it was already pointed out that these classes are due to variations in the accretion rates. Chakrabarti et al. (2004a) reported some of the actual class transitions using observations with IXAE. They showed that these transitions are smooth and in between two ‘known’ classes the object stays in an ‘unknown’ classes. In Chakrabarti et al. (2004b), a few other class transitions are reported and it was further established that during a class transition, the photon count changes considerably and it is possible to understand this behaviour by assuming changes in the sub-Keplerian accretion rate.

To begin with we present the classes as presented by Belloni et al. (2000) in a sequence which is easier to understand using TCAF. Figure 5 (Nandi et al. 2000) shows the twelve classes marked by 1...12 which are called χ , α , ν , β , λ , κ , ρ , μ , θ , δ , γ and ϕ respectively. Panels 3 and 6 have more than one light curve (separated by dashed line), as they are similar but with subtle difference. Along X-axis is the time elapsed in seconds since the beginning of the

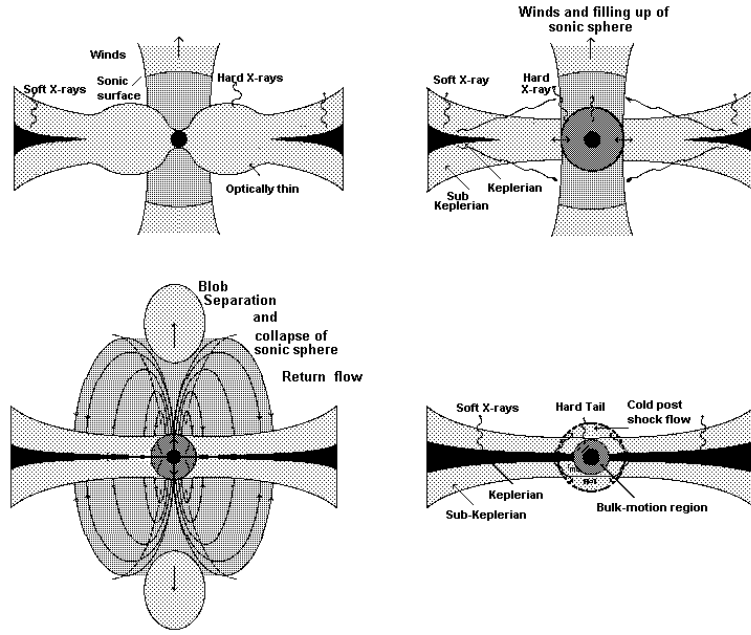


Fig. 3 Typical configurations of the two component advective flows around a black hole. See text for details.

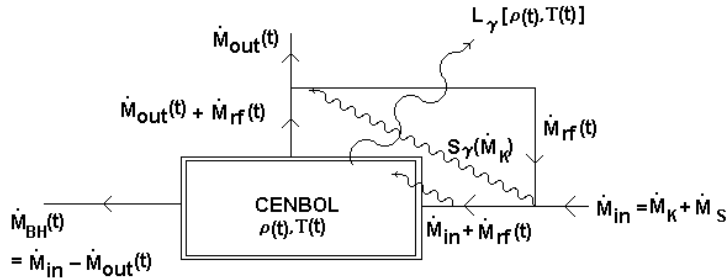


Fig. 4 Schematic diagram of the interaction of the boundary layer (CENBOL) and the outflow with the radiation emitted from the accretion flow. If the radiation is strong, outflow is quenched (Chakrabarti et al. 2002b).

observation. Spectral analysis of the 1st panel suggests that it is purely in hard state. There is a prominent QPO whose frequency may change from time to time and photon count number may also change significantly. Final three panels (10–12) contain light curves of those days on which spectral states are soft. There are no QPOs in these days. Spectral fits indicate high temperature and high photon spectral index. The ninth panel contains a light curve where two semi-soft spectra with different photon counts are seen. Count rate varies very significantly. In the remaining seven panels, (2–8) photons jump in between two distinct states, one with a low photon count (off state) and the other with a high photon count (on state).

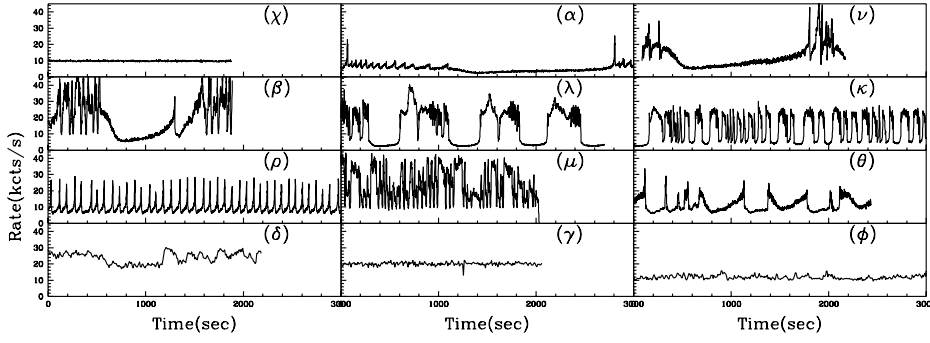


Fig. 5 Classification of major light curves (Belloni et al. 2000) according to various colour-colour diagrams.

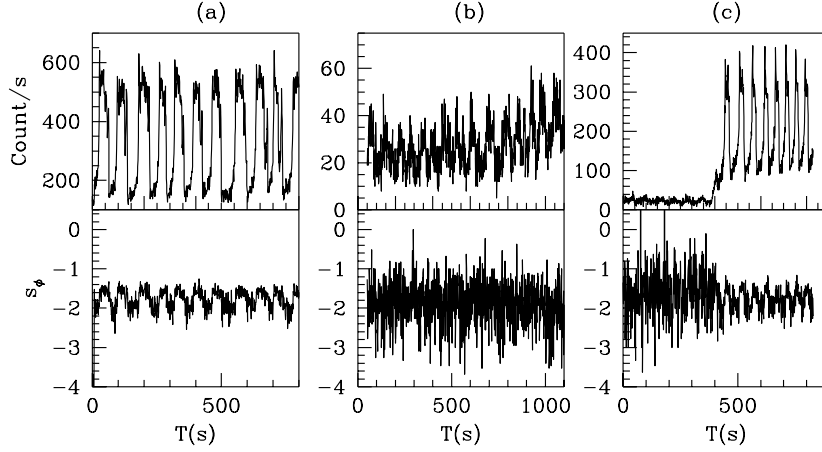


Fig. 6 Light curves (2–18 keV) as observed by IXAE (upper panel) and the mean photon spectral index s_ϕ (lower panel) in the 1st, 3rd and 5th orbits of June 22nd, 1997. GRS1915+105 was in the κ class in (a), in an unknown class in (b) and went to the ρ class in (c) on that day. From Chakrabarti et al. (2004b).

In Fig. 6(a-c), we present a few examples of the class transition (Chakrabarti et al 2004b). We present the light curves (2–18 keV) of June 22nd, 1997 observation in the upper panel and the mean photon index (MPI) in the lower panels. The MPI s_ϕ is obtained using the definition: $s_\phi = -\frac{\log(N_{6-18}/E_2) - \log(N_{2-6}/E_1)}{\log(E_2) - \log(E_1)}$ where, N_{2-6} and N_{6-18} are the number of photons from the top layer of the PPC and $E_1 = 4$ and $E_2 = 12$ are the mean energies in each channel. The Fig. 6a is in the so-called k class. The Fig. 6b is in an unknown class and the Fig. 6c clearly shows the transition from the unknown class to the so-called ρ class. The panels are separated by about three hours.

In the lower panels, the s_ϕ oscillates between ~ 2.4 to ~ 1.4 in Fig. 6b and in Figs. 6b and 6c, the unknown class produced very noisy photon spectral slope variation. As soon as the ρ class is achieved after one ‘semi- ρ ’ oscillation, noise in s_ϕ is reduced dramatically.

In Fig. 7(a-b), we show light curve and s_ϕ from IXAE data obtained on the 8th of June, 1999 (Chakrabarti et al 2004a). The two panels are from two successive orbits ~ 80 minutes apart. In Fig. 7a, the power density spectrum (PDS) is typical of that of the χ class but the count rate

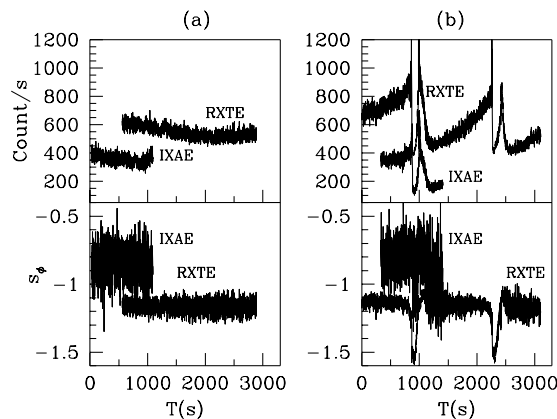


Fig. 7 Class transition as seen from IXAE and RXTE observations on the 8th of June, 1999 in two successive orbits (marked). RXTE photon counts are divided by 50 and shifted upward by 200/s for comparison. In (a), no significant variation in light curve or spectral index and the object was in χ -like class with high counts. In (b), the object is distinctly in the θ class. There is a gap of 44 minutes in the two RXTE data presented in (a) and (b). From Chakrabarti et al. (2004b).

was very high compared to what is expected from such a class. A QPO at 4.7 Hz is present. The s_ϕ is 0.85 which is harder than what is observed in Fig. 6. When combined with RXTE data of that date (Fig. 7a), one finds that for a long time (~ 3000 s) there was no signature of any ‘dip’ — the characteristic of the θ class. Hence, this must be in an unknown class, more close to χ than any other. RXTE also observed this object on 7th of June, 1999 and found the object to be in the χ class. In Fig. 7b, the light curve in the next orbit of IXAE shows the evidence of the so-called θ class. Interestingly, the spectra gradually ‘hardened’ to $s_\phi \sim 0.6$ just before the ‘dip’. The spectra characteristically softened in the ‘dip’ region with $s_\phi \sim 1.4$ as the inner edge of the disk is disappeared. This class transition is confirmed in the data of RXTE also shown in Fig. 7b. The lower panels showed that the spectral slopes obtained for RXTE data calculated in the similar way as s_ϕ was calculated before. Here, the RXTE photons were first binned in 2–6 keV and 6–15 keV energies before computing s_ϕ from $s_\phi = -\frac{\log(N_{6-15}/E_2) - \log(N_{2-6}/E_1)}{\log(E_2) - \log(E_1)}$, where, $E_1 = 4$ keV, $E_2 = 9$ keV.

4 EXAMPLES OF POSSIBLE CLASS TRANSITIONS IN OTHER OBJECTS

Though the variability classes have not been studied for other objects as was done for GRS 1915+105, there are some evidence that the emitted radiation changes specific characteristics in short time periods. In Fig. 8(a-b) we show peculiar features in RXTE light-curves (Nespoli et al. 2003) of GX339-4 taken on MJD 52411 (May 17th, 2002) in two successive orbits. In Fig. 8a, the light curves in the upper panel and the color (ratio of counts in the 16.4-19.8 bands over 3.7-6.5keV bands) in the lower panel are shown. Power density spectra indicated presence of a QPO at ~ 6 Hz in the second orbit. Detailed study showed that there was no QPO for first two minutes or so into of observation of the second orbit, and then the QPO appeared with variable frequency (Fig. 8b). The appearance of QPOs indicate the formation of an oscillating shock (see Fig. 3, upper-right panel), which is induced by the resonance in cooling time-scale and the infall time-scales from the post-shock flow (Molteni, Sponholz & Chakrabarti, 1996).

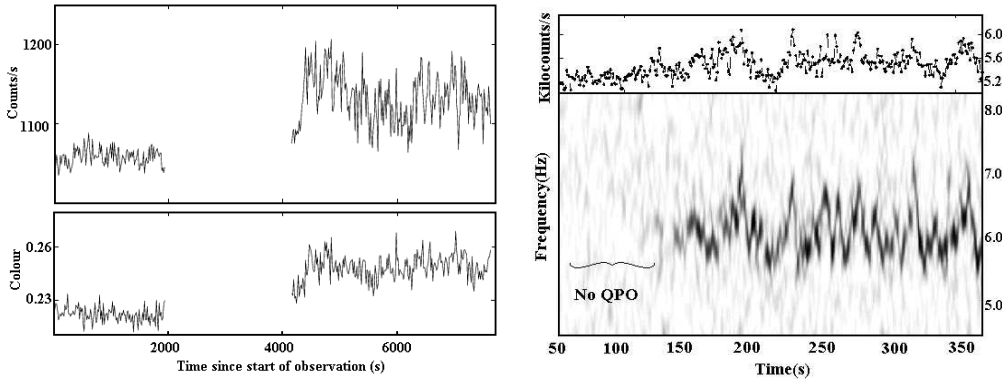


Fig. 8 Example of a transition of some kind in GX339-4 as is evident from the (a) lightcurve and colour variation in two successive orbits and the (b) averaged counts and dynamical PDS of the second orbit. QPO appears after a couple of minutes of the beginning of the second orbit indicating the change in flow configuration from a no-shock or steady shock flow to an oscillating shock flow (Figures adapted from Nespoli et al., 2003).

This resonance could be short lived or transient, since the accretion rate was changing during this observation. More such observations would be essential to classify the nature of variations.

Another example can be provided for GRO 1655-40 in which the state transition has been observed (Sobczak et al. 1999, Remillard et al. 1999). Figure 9(a-b) shows the spectra at four times with the following PIDs: (i) 20402-02-02-00 (Mar. 05, 1997) to represent high/soft state (lower-right panel of Fig. 3), (ii) 20402-02-25-00 (Aug. 14, 1997) to represent an intermediate hard-state which is losing matter to the sonic sphere (early stage of lower-left panel of Fig. 3), (iii) 20402-02-24-00 (Aug. 03, 1997) to represent an intermediate soft state just before the state transition (late stage of lower-left panel of Fig. 3) and finally (iv) 20402-02-26-00 (Aug. 18th, 1997) to represent a true hard state (upper right panel of Fig. 3). We fitted the spectra keeping the hydrogen column density fixed at 0.89×10^{22} atoms per cm^{-2} (Zhang et al. 1997). According to the theoretical understanding (Chakrabarti, 1999; 2002b), one should expect case (iii) to have harder spectra compared to case (i) and case (ii) to have a softer spectra compared to case (iv). That is precisely seen in Figs. 9a and 9b respectively. There is no evidence for QPO in both the soft states (Fig. 9a) while a strong QPO is observed in case (ii) at 1.4 Hz and 6.4 Hz while a weak QPO is observed in case (iv) at 0.2 Hz and 0.8 Hz (Fig. 9b). If oscillation of shocks correspond to QPOs (Molteni, Sponholz & Chakrabarti, 1996; Chakrabarti & Manickam, 2000) and if shocks also produce outflows (Chakrabarti, 1999) then it is clear that a strong shock (and therefore outflow) is present in case (ii) while there is a weak shock very far out (since $\nu_{\text{QPO}} \propto R_s^{3/2}$, where R_s is the shock location) in case (iv).

The softening of the hard state and the hardening of the soft state spectra have been found to be related to the presence of outflow and return flow respectively (Chakrabarti et al. 2002b). These phenomena occur because when matter goes out of the CENBOL the number of electrons go down for the same source of soft photons and the spectrum is softened. Conversely, when matter returns back, the spectrum is hardened. as a result, the pivotal point between the burst-on and burst-off states (where the wind activity is prominent) shifts outward by a few keV as compared to the pivotal point between the hard and soft states (when the wind activity is relatively lower). This phenomenon is routinely observed in GRS 1915+105. Figures 10(a-c) show the comparison of spectra in burst-on and burst off states of (a) June 18, 1997, (b) July

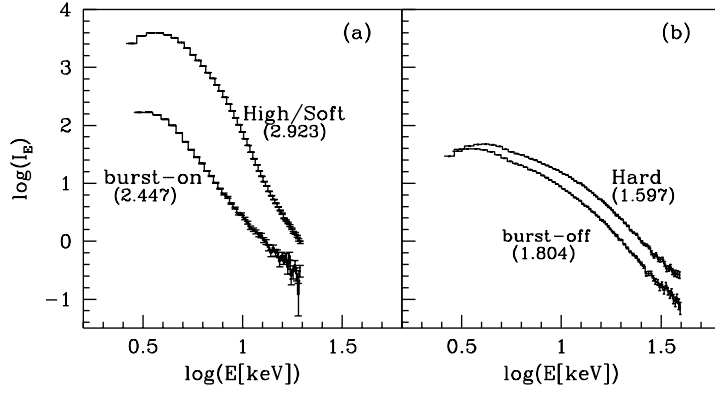


Fig. 9 Comparison of spectra of (a) high and burst-on and (b) low and burst-off phases of GRO 1655-40 clearly showing hardening of the soft state and softening of the hard state. From Chakrabarti et al. (2002b).

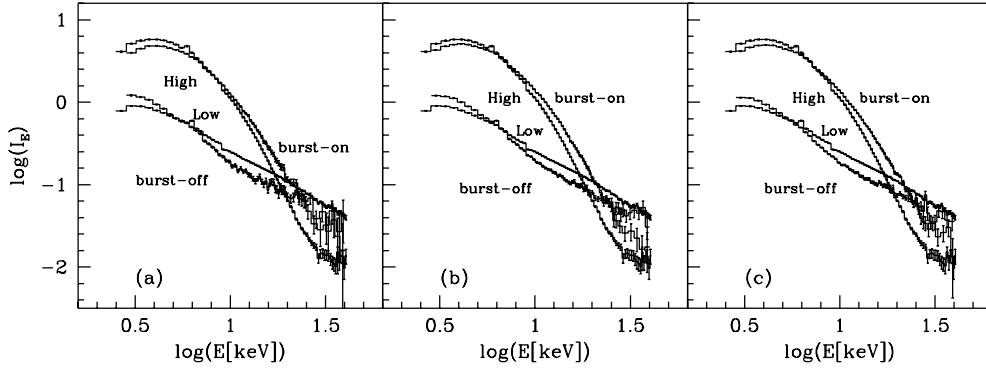


Fig. 10 Comparison of the spectra of GRS 1915+105 on three different days with generic high (typically ϕ) and low (typically ϕ) state spectra of the same source to indicate that variability class transition to burst-off/burst-on (typically, λ or κ) is also accompanied by shifting of the pivotal energy. From Chakrabarti et al (2002b).

10, 1997 and (c) July 12, 1997 respectively. The spectra in the high and the low states for the same object on August 19, 1997 and March 26, 1997 respectively are plotted to establish the shifting of the pivotal point in presence of winds.

5 CONCLUDING REMARKS

Variability class transitions are common in GRS 1915+105 and probably have been seen in GX 339-4 and GRO 1655-40. For a given black hole, there are only two parameters, namely, the accretion rate of the Keplerian component and that of the sub-Keplerian halo which can give rise to these transitions. Alternatively, if one assumed that both the matter is supplied at the outer edge of the disk, then this accretion rate together with the viscosity parameter ($\alpha(r, z)$) should be enough. In the TCAF solution, the separation of the Keplerian from sub-Keplerian can be achieved by appropriate viscosity parameters, and hence independent variation of the two rates produces the same result.

We presented a few examples of the class transitions in GRS 1915+105 especially using the IXAE experiment aboard IRS P3. The count rate was found to change before and during class transition and the two classes before and after the transition were not found to have ‘normal’ counts characteristics of those classes. The transition also occurs via an unknown class. It takes about 2-3 hours for a transition which may typically be the free-fall time-scale of the low-angular momentum (sub-Keplerian) flow. Thus, it is possible that the major cause of transition is the slow change in the accretion rates.

The transitions discussed in this review are related to the galactic black holes only. For extra-galactic black holes, the same phenomenon is expected, but on a quite longer time-scale (as each time interval scales with the mass of the central hole) and it is not clear if this has been observed yet.

Acknowledgements This work was partly supported by the DST project ‘Emitted Spectra from Two-Component Accretion Disks Around Black Holes’.

References

- Belloni T. et al., 2000, *A&A*, 355, 271
 Chakrabarti S. K., 1990, *Theory of Transonic Astrophysical Flows*, (World Scientific: Singapore)
 Chakrabarti S. K., 1993, *Numerical Simulations in Astrophysics*, J. Franco et al. (Eds.), Mexico city, Mexico (Cambridge University Press:UK)
 Chakrabarti S. K., 1994, *Proceedings of 17th Texas Symposium In H. Böhringer et al. (Eds.), Munich, Germany, New York Academy of Sciences, New York*
 Chakrabarti S. K., 1996, *Physics Reports*, Vol. 266, Nos.5 & 6, 229
 Chakrabarti S. K., 1998, *Ind. J. Phys.*, 72(B), 565
 Chakrabarti S. K., 1999, *Astron. & Astrophys.*, 351, 185
 Chakrabarti S. K., 2001, *Astrophys. and Space Science*, 276, 191
 Chakrabarti S. K., Acharyya K., Molteni D., 2004, *A&A*, 421, 1
 Chakrabarti S. K., Manickam S. G., 2000, *ApJ* 531, L41
 Chakrabarti S. K., Manickam S. G., Nandi A., Rao A. R., 2002, in the *Proceedings of the IXth Marcel Grossman Meeting*, Eds. V. G. Gurzadyan, R. T. Jantzen, R. Ruffini, (World Scientific Co.: Singapore), 2279
 Chakrabarti S. K., Molteni D., 1995, *MNRAS*, 272, 80
 Chakrabarti S. K., Nandi A., 2000, *Ind. J. Phys.*, 75(B), 1
 Chakrabarti S. K., Nandi A., Choudhury A., Chatterjee U., 2004a, *ApJ*, 607, 406
 Chakrabarti S. K., Nandi A., Chatterjee A. K., Choudhury A., Chatterjee U., 2004b, *A&A*, 431, 825
 Chakrabarti S. K., Nandi A., Manickam S. G., Mandal S., Rao A. R., 2002b, *ApJ*, 579, L21
 Chakrabarti S. K., Titarchuk L. G., 1995, *ApJ*, 455, 623
 Molteni D., Sponholz H., Chakrabarti S. K., 1996, *ApJ*, 457, 805
 Naik S., Rao A. R., Chakrabarti S. K., 2002a, *J. Astron. Astrophys*, 23, 213
 Nespoli E., et al., 2003, *A&A*, 412, 235
 Remillard R. A., Morgan E. H., McClintock J. E., Bailyn C. D., Orosz J. A., 1999, *ApJ*, 522, 397
 Shapiro S. L., Lightman A. P., Eardley D. M., 1976, *ApJ*, 204, 187
 Smith D. M., Heindl W. A., Swank J. H., 2002, *ApJ*, 569, 362
 Sobczak G. J., McClintock J. E., Remillard R. A., Bailyn C. D., Orosz J. A., 1999, *ApJ*, 520, 776
 Zhang S. N., et al. 1997, *ApJ*, 479, 381